TRAF2 is a biologically important necroptosis suppressor

SL Petersen[1], TT Chen[1], DA Lawrence[1], SA Marsters[1], F Gonzalvez[1] and A Ashkenazi*,[1]

Tumor necrosis factor α (TNFα) triggers necroptotic cell death through an intracellular signaling complex containing receptor-interacting protein kinase (RIPK) 1 and RIPK3, called the necrosome. RIPK1 phosphorylates RIPK3, which phosphorylates the pseudokinase mixed lineage kinase-domain-like (MLKL)—driving its oligomerization and membrane-disrupting necroptotic activity. Here, we show that TNF receptor-associated factor 2 (TRAF2)—previously implicated in apoptosis suppression—also inhibits necroptotic signaling by TNFα. TRAF2 disruption in mouse fibroblasts augmented TNFα–driven necrosome formation and RIPK3-MLKL association, promoting necroptosis. TRAF2 constitutively associated with MLKL, whereas TNFα reversed this via cylindromatosis-dependent TRAF2 deubiquitination. Ectopic interaction of TRAF2 and MLKL required the C-terminal portion but not the N-terminal, RING, or CIM region of TRAF2. Induced *TRAF2* knockout (KO) in adult mice caused rapid lethality, in conjunction with increased hepatic necrosome assembly. By contrast, *TRAF2* KO on a *RIPK3* KO background caused delayed mortality, in concert with elevated intestinal caspase-8 protein and activity. Combined injection of TNFR1-Fc, Fas-Fc and DR5-Fc decoys prevented death upon *TRAF2* KO. However, Fas-Fc and DR5-Fc were ineffective, whereas TNFR1-Fc and interferon α receptor (IFNAR1)-Fc were partially protective against lethality upon combined *TRAF2* and *RIPK3* KO. These results identify TRAF2 as an important biological suppressor of necroptosis *in vitro* and *in vivo*.
Cell Death and Differentiation (2015) **22,** 1846–1857; doi:10.1038/cdd.2015.35; published online 17 April 2015

Apoptotic cell death is mediated by caspases and has distinct morphological features, including membrane blebbing, cell shrinkage and nuclear fragmentation.[1–4] In contrast, necrotic cell death is caspase-independent and is characterized by loss of membrane integrity, cell swelling and implosion.[1,2,5] Nevertheless, necroptosis is a highly regulated process, requiring activation of RIPK1 and RIPK3, which form the core necrosome complex.[1,2,5] Necrosome assembly can be induced via specific death receptors or toll-like receptors, among other modules.[6–9] The activated necrosome engages MLKL by RIPK3-mediated phosphorylation.[6,10,11] MLKL then oligomerizes and binds to membrane phospholipids, forming pores that cause necroptotic cell death.[10,12–15] Unchecked necroptosis disrupts embryonic development in mice and contributes to several human diseases.[7,8,16–22]

The apoptotic mediators FADD, caspase-8 and cFLIP suppress necroptosis.[19–21,23,24] Elimination of any of these genes in mice causes embryonic lethality, subverted by additional deletion of *RIPK3* or *MLKL*.[19–21,25] Necroptosis is also regulated at the level of RIPK1. Whereas TNFα engagement of TNFR1 leads to K63-linked ubiquitination of RIPK1 by cellular inhibitor of apoptosis proteins (cIAPs) to promote nuclear factor (NF)-κB activation,[26] necroptosis requires suppression or reversal of this modification to allow RIPK1 autophosphorylation and consequent RIPK3 activation.[2,23,27,28] CYLD promotes necroptotic signaling by deubiquitinating RIPK1, augmenting its interaction with RIPK3.[29] Conversely, caspase-8-mediated CYLD cleavage inhibits necroptosis.[24]

TRAF2 recruits cIAPs to the TNFα-TNFR1 signaling complex, facilitating NF-κB activation.[30–33] TRAF2 also supports K48-linked ubiquitination and proteasomal degradation of death-receptor-activated caspase-8, curbing apoptosis.[34] *TRAF2* KO mice display embryonic lethality; some survive through birth but have severe developmental and immune deficiencies and die prematurely.[35,36] Conditional *TRAF2* KO leads to rapid intestinal inflammation and mortality.[37] Furthermore, hepatic TRAF2 depletion augments apoptosis activation via Fas/CD95.[34] TRAF2 attenuates necroptosis induction *in vitro* by the death ligands Apo2L/TRAIL and Fas/CD95L.[38] However, it remains unclear whether TRAF2 regulates TNFα-induced necroptosis—and if so—how. Our present findings reveal that TRAF2 inhibits TNFα necroptotic signaling. Furthermore, our results establish TRAF2 as a biologically important necroptosis suppressor *in vitro* and *in vivo* and provide initial insight into the mechanisms underlying this function.

Results

Loss of TRAF2 promotes TNFα-induced necroptosis. To investigate whether TRAF2 regulates necroptosis, we first

[1]Cancer Immunology, Genentech, Inc., 1 DNA Way, South San Francisco, CA 94080, USA
*Corresponding author: A Ashkenazi, Cancer immunology, Genentech, Inc., 1 DNA Way, MS 42, South San Francisco, CA 94080-4918, USA. Tel: +1 650 225 1853; Fax: +1 650 467 8195; E-mail: aa@gene.com
Abbreviations: CHX (C), cycloheximide; cIAP, cellular inhibitor of apoptosis protein; CYLD, cylindromatosis; FADD, Fas-associated death domain; IFN, interferon; MEF, mouse-embryo fibroblast; MLKL, mixed lineage kinase domain-like; Nec-1 (N), necrostatin-1; NF-κB, nuclear factor-κB; RIPK1, receptor interacting protein kinase 1; RIPK3, receptor interacting protein kinase 3; TNFα (T), tumor necrosis factor α; TRAF2, TNF receptor-associated factor 2; Ub, ubiquitin; Z-VAD-fmk (Z), benzyloxycarbonyl-Val-Ala-Asp(OMe)-fluoromethylketone
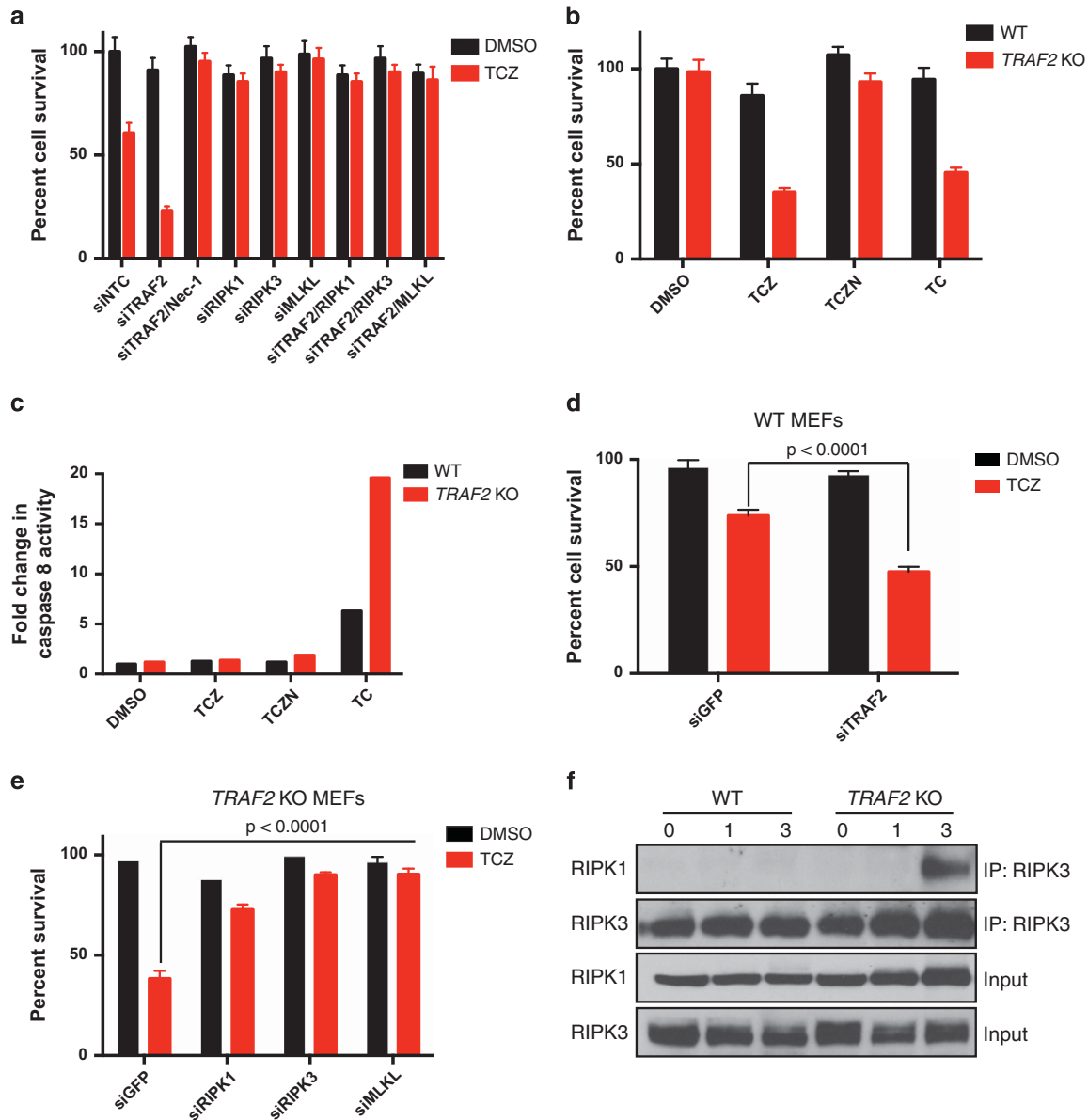
Figure 1 Loss of TRAF2 augments TNFα-induced necroptosis. (**a**) L929 cells were transfected for 3 days with siRNA as indicated. Cells were then pretreated for 1 h with zVAD (Z) (20 μM), cycloheximide (**c**) (1 μg/ml) and necrostatin-1 (N) (20 μM) for 1 h followed by TNFα (T) (100 ng/ml) for an additional 5 h. Cell survival was determined by measuring ATP consumption using Cell Titer Glo assay. (**b**, **c**) WT and *TRAF2* KO MEFs were treated and analyzed for viability (**b**) or for caspase-8 activity (**c**). (**d**, **e**) WT and *TRAF2* KO MEFs were transfected with siRNA for 3 days, subjected to the indicated treatments and analyzed for survival. (**f**) WT and *TRAF2* KO MEFs were treated with TCZ as above for the indicated times and analyzed by immunoprecipitation (IP) followed by immunoblot (IB) for proteins indicated on the left. Data in panels **a–e** represent mean $\pm$ S.E.M. ($n = 4$). *P* values are by Student's *t* test

depleted it by siRNA transfection in mouse L929 fibrosarcoma cells.[39] TRAF2 knockdown significantly augmented TNFα-induced necroptosis, evident by loss of cell viability in the presence of TNFα plus the translation inhibitor CHX and the pan-caspase inhibitor Z-VAD-fmk (TCZ); and by inhibition of cell death by the RIPK1 inhibitor Nec-1 (Figure 1a). Additional siRNA knockdown of RIPK1, RIPK3 or MLKL reversed the augmentation (Figure 1a and Supplementary Figures 1A and B), confirming necroptosis suppression.

To rule out potential off-target TRAF2 siRNA effects, we turned next to *TRAF2* KO MEFs. *TRAF2* KO MEFs were much

more responsive to TCZ-induced death than were wild-type (WT) MEFs (Figure 1b). Nec-1 blocked cell death in both cases, verifying necroptosis augmentation upon *TRAF2* deletion. In the absence of Z-VAD (TC), *TRAF2* KO MEFs showed stronger TNFα-induced cell death and caspase-8 activation than did WT MEFs (Figures 1b and c), consistent with earlier evidence that TRAF2 suppresses cell-extrinsic apoptotic signaling.[34,40] TRAF2 siRNA knockdown in WT MEFs also enhanced TNFα-induced necroptosis (Figure 1d and Supplementary Figure 1C). Knockdown of RIPK1, RIPK3 or MLKL attenuated TCZ-induced death in *TRAF2* KO MEFs, suggesting that *TRAF2* regulates necroptosis via the

RIPK1-RIPK3-MLKL pathway (Figure 1e and Supplementary Figures 1D and E). *TRAF2* KO MEFs formed a readily detectable necrosome, evident by co-immunoprecipitation (co-IP) of RIPK3 within 3 h of TCZ treatment (Figure 1f and

Supplementary Figures 1F and G); WT MEFs assembled a weaker necrosome by 6 h (Supplementary Figure 1H). Knockdown of TRAF2 in L929 cells similarly augmented RIPK1-RIPK3 association (Supplementary Figure 1I). Thus,
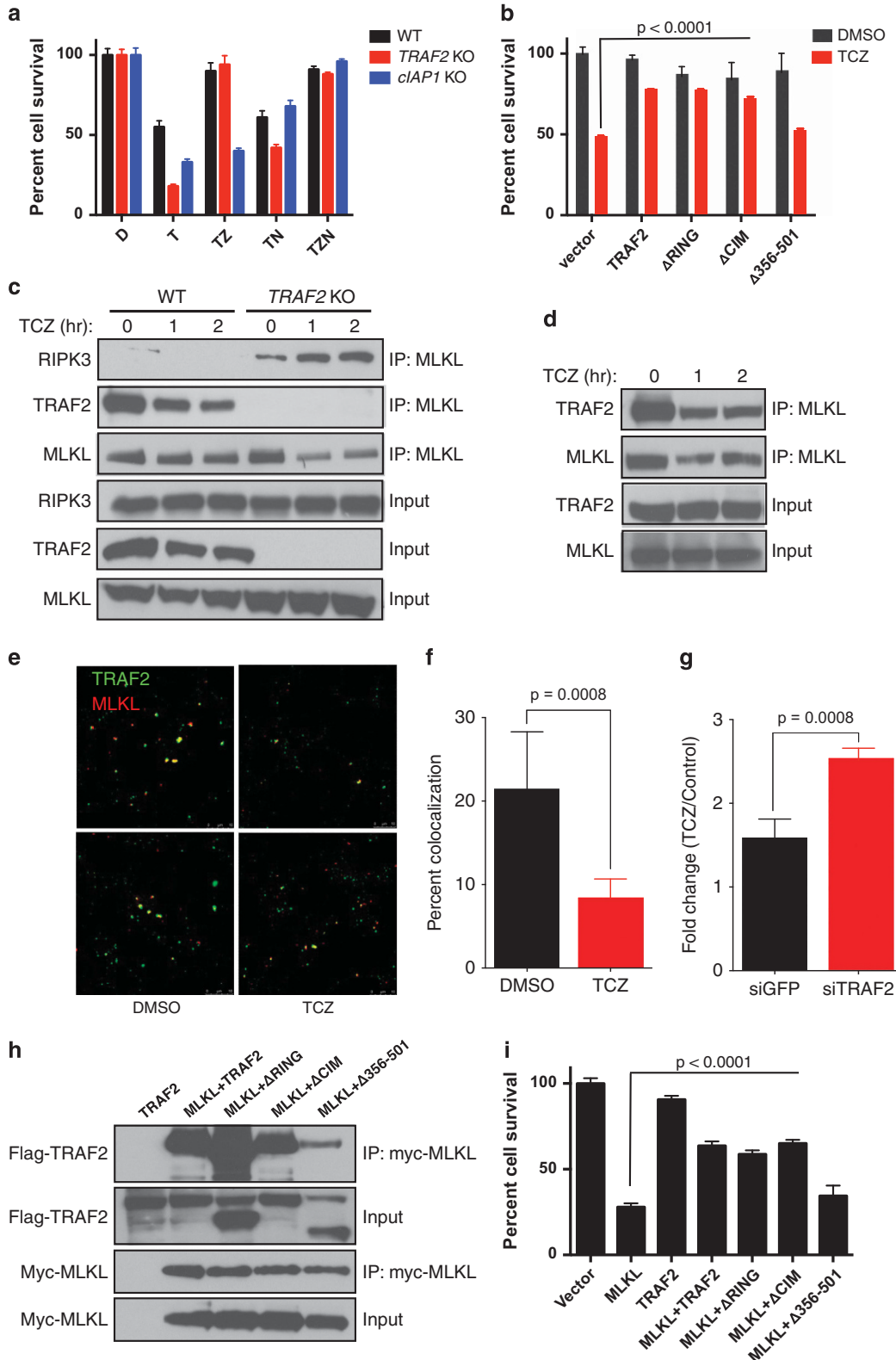
TRAF2 depletion in murine fibroblasts augments TCZ-induced necrosome assembly and necroptosis, suggesting that at least one level of signal suppression by TRAF2 is upstream of the necrosome.

Evidence for a constitutive interaction of TRAF2 with MLKL. Although in the absence of CHX TNFα did not induce detectable cell death in WT MEFs at 5 h (data not shown), it decreased cell viability by ~ 50% within 24 h (Figure 2a). Both *TRAF2* KO and *cIAP1* KO MEFS showed greater sensitivity to TNFα than did WT MEFs; however, whereas Z-VAD fully blocked TNFα-induced death in *TRAF2* KO MEFs, it provided little protection in *cIAP1* KO MEFs. Conversely, Nec-1 inhibited TNFα-induced death more strongly in *cIAP1* KO as compared with *TRAF2* KO MEFs. Thus, in response to TNFα without CHX, *TRAF2* KO favors apoptosis, whereas *cIAP1* KO supports necroptosis, suggesting that that TRAF2 modulates necroptosis not only via cIAPs but also at some additional level(s).

Transfection of *TRAF2* KO MEFs with a TRAF2 deletion mutant lacking the RING domain suppressed TNFα-induced necroptosis as effectively as did reconstitution with WT *TRAF2* (Figure 2b and Supplementary Figure 2A). Hence, unlike apoptosis inhibition,[34] necroptosis suppression by TRAF2 is RING-independent. A TRAF2 mutant lacking the cIAP-interaction motif (CIM)[30,41] was similarly effective at attenuating the effect of *TRAF2* KO, consistent with the notion that TRAF2 also operates independently of cIAP binding. In contrast, deletion of the C-terminal portion of TRAF2 (aa 356-501) did not significantly rescue the *TRAF2* KO phenotype.

In light of previous work suggesting that TRAF2 is capable of binding MLK3,[42] we examined whether TRAF2 also interacts with MLKL. IP of MLKL from *WT* MEFs revealed association with TRAF2 at baseline, whereas TCZ treatment decreased this interaction by ~ 50% over 2 h (Figure 2c and Supplementary Figures 2B–D). We detected minimal baseline RIPK3-MLKL interaction in *WT* MEFs; however, in *TRAF2* KO MEFs, RIPK3 and MLKL showed some interaction without stimulation—and this increased significantly upon TCZ treatment, in concert with apparent dissociation of TRAF2 from MLKL (Figure 2c). TRAF2 similarly associated with MLKL in L929 cells, whereas TCZ treatment substantially decreased this interaction (Figure 2d). Consistent with earlier data,[10] we could not detect RIPK3-MLKL binding in L929 cells.

In keeping with the co-IP data (Figure 2d), immunofluorescence analysis of L929 cells revealed ~ 20% co-localization of TRAF2 and MLKL at baseline, whereas TCZ treatment decreased this by ~ 2.5-fold (Figure 2e and Supplementary Figure 2E). Furthermore, siRNA knockdown of TRAF2

increased the co-localization between RIPK3 and MLKL by ~ 2.5-fold (Figures 2f and g). Thus, TRAF2 may associate with MLKL at baseline, whereas TNFα stimulation may reverse this in concert with increased RIPK3-MLKL binding, suggesting that TRAF2 association suppresses the interaction of MLKL with RIPK3.

To examine which part of the TRAF2 protein is required for MLKL interaction, we transfected 293T cells with vectors encoding myc-epitope-tagged MLKL together with WT or deletion variants of TRAF2. IP of MLKL via myc revealed association with WT TRAF2 or its RING- or CIM-deletion variants, but not the TRAF2 C-terminal-deletion mutant (Figure 2h). Transfection of MLKL, but not of TRAF2, induced marked cell death (Figure 2i); importantly, co-transfection of MLKL with WT TRAF2 or its RING- or CIM-deletion variants (which retained MLKL binding) substantially blocked cell-death induction, whereas co-transfection with the C-terminal-deletion mutant (which failed to bind MLKL) did not. Cells co-transfected with MLKL and TRAF2 expressed less TRAF2 than did cells transfected with TRAF2 alone, perhaps owing to decreased viability upon MLKL overexpression. Regardless, the C-terminal portion of TRAF2 appears specifically important for MLKL association and for effective necroptosis suppression.

CYLD is required for TRAF2 deubiquitination and dissociation from MLKL. We examined whether the ubiquitination state of TRAF2 affects its apparent interaction with MLKL. IP of TRAF2 from L929 cells under denaturing conditions—to eliminate associated proteins—followed by immunoblot (IB) for ubiquitin, revealed abundant TRAF2 ubiquitination at baseline; however, TCZ treatment completely reversed this within 2 h (Figure 3a). Albeit less robustly, IP of TRAF2 from WT MEFs also indicated basal TRAF2 ubiquitination, which decreased upon TCZ treatment (Supplementary Figure 3A); in contrast, TRAF2 IP from *TRAF2* KO MEFs did not show any ubiquitination. IP of RIPK1 indicated RIPK1 association with TRAF2 within 1 h of TCZ treatment, followed by dissociation by 2 h (Supplementary Figure 3B), consistent with TNFR1 recruitment and release of RIPK1. As expected, RIPK1 IP revealed its transient ubiquitination, appearing 1 h after TCZ addition and declining by 2 h (Supplementary Figure 3C).

CYLD promotes TNFα-induced necroptosis by deubiquitinating RIPK1,[29] yet inhibits CD40 signaling to NF-κB by deubiquitinating TRAF2.[43,44] To determine whether CYLD regulates TRAF2 in the context of TNFα-induced necroptosis, we depleted CYLD by siRNA in L929 cells. Whereas TCZ treatment induced TRAF2 deubiquitination, CYLD knockdown

---

Figure 2 TRAF2 constitutively interacts with MLKL to suppress necroptosis. (**a**) WT, *TRAF2* KO and *cIAP1* KO MEFs were treated as indicated for 1 day and analyzed for survival. (**b**) *TRAF2* KO MEFs were transfected with the indicated expression constructs for 2 days, pretreated with CZ for 1 h followed by T for an additional 5 h, and analyzed for survival. (**c**) WT and *TRAF2* KO MEFs were treated as in **b** for the indicated times and analyzed by IP and IB. (**d**) L929 cells were treated as in **c** and analyzed by IP and IB. (**e**) L929 cells were treated as indicated for 90 min and analyzed by immunofluorescence (IF) with specific antibodies to TRAF2 (green) or MLKL (red). (**f**) Quantitation of IF data generated as in **e**. (**g**) L929 cells were transfected for 3 days with siRNA as indicated, treated with DMSO or TCZ for 90 min, analyzed by IF as in **e** and the data was quantitated ($n = 3$) and depicted as fold change from DMSO control levels. (**h**) 293T cells were transfected with constructs encoding myc-epitope-tagged MLKL, WT TRAF2 or indicated TRAF2 deletion mutants for 1 day followed by myc IP and TRAF2 IB. (**i**) 293T cells were transfected as in **h** for 2 days and analyzed for survival. Bar graphs in **i** depict mean $\pm$ S.E.M. of triplicates. Data in panels **a**, **b** depict mean $\pm$ S.E.M. ($n = 4$). For colocalization studies (panels **f** and **g**) three independent experiments were performed and six images for each treatment were quantified. *P* values are by Student's *t* test

reversed this effect and stabilized the association of TRAF2 with MLKL (Figures 3b and c). In keeping with earlier data,[29] CYLD knockdown provided complete protection against TNF*α*-induced necroptosis (Figure 3d). Importantly, CYLD depletion also blocked cell-death augmentation by TRAF2 knockdown (Figure 3d). Furthermore, whereas cIAP1-mediated *in vitro* ubiquitination of recombinant (r) TRAF2 supported binding to rMLKL, addition of rCYLD reversed rTRAF2 ubiquitination and partially inhibited rTRAF2 binding to rMLKL (Supplementary Figure 3D). Thus, TRAF2 deubiquitination by CYLD promotes the dissociation of TRAF2 from MLKL.

TRAF2 KO is lethal in adult mice. Mouse embryonic lethality of *TRAF2* KO has been ascribed to deficient NF-*κ*B signaling and excessive apoptosis.[35,36] The observation that loss of *TRAF2* augments necroptosis *in vitro* prompted us to investigate whether elevated necroptosis also contributes to *in vivo* mortality upon deletion of *TRAF2*. To examine this, we generated inducible *TRAF2* KO mice via a *TRAF2 loxp/loxp. RosaCreERTS* gene construct (see Methods). To induce ubiquitous *TRAF2* deletion, we treated mature mice with tamoxifen at 40 or 80 mg/kg daily for 5 days by intraperitoneal injection. All tamoxifen-treated mice displayed severe weight loss, deterioration in vital appearance of the liver and gastrointestinal system, and moribund behavior; these mice died or had to be killed within 1–3 days following final tamoxifen injection (Figures 4a and c). To rule out potential off-target effects of tamoxifen, we compared cre-negative and cre-positive mice possessing both loxp sites. In response to tamoxifen (40 mg/kg), cre-negative mice displayed no adverse reactions, whereas cre-positive mice lost significant
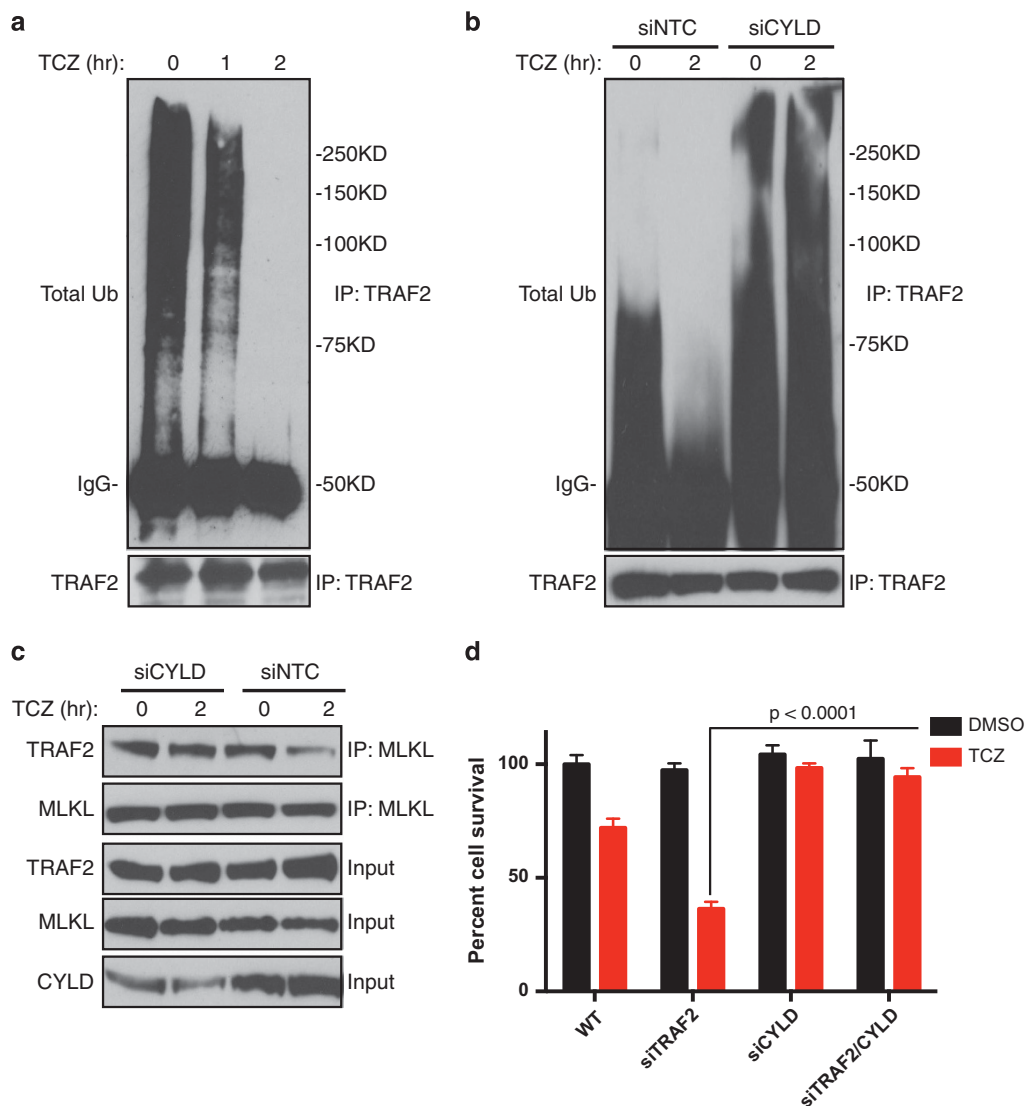

Figure 3 CYLD mediates TRAF2 deubiquitination and dissociation from MLKL. (**a**) L929 cells were treated for with CZ for 1 h followed by T for the indicated times. Cells were lysed in 1.5% SDS, diluted to 0.15% in SDS-PAGE buffer and analyzed by TRAF2 IP followed by IB with anti-ubiquitin (Ub) antibody. (**b**) L929 cells were transfected with siRNA as indicated for 3 days followed by treatment and analysis as in **a**. (**c**) L929 cells were transfected as in **b**, pretreated with CZ for 1 h followed by T for indicated times, and analyzed by IP and IB. (**d**) L929 cells were transfected as in **b**, treated with CZ for 1 h followed with T for 5 h, and analyzed for survival. Data in **d** depict mean $\pm$ S.E.M. ($n = 4$). *P* values are by Student's *t* test
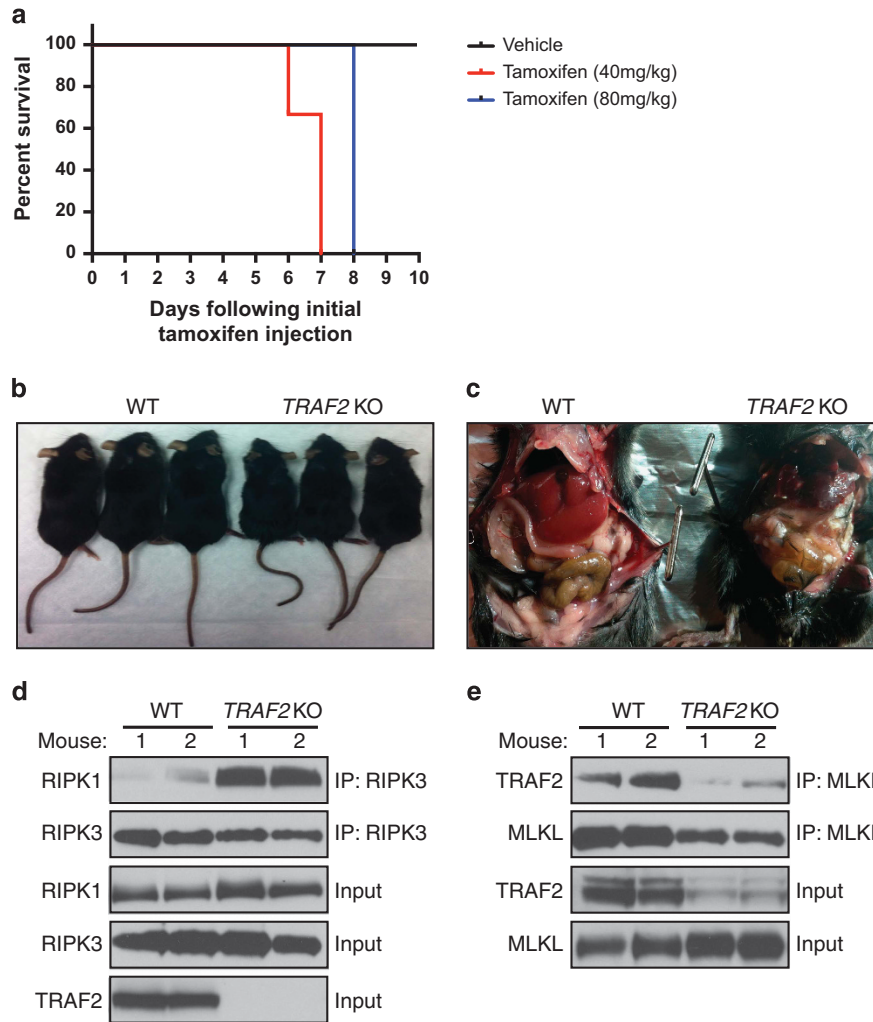
Figure 4 Inducible *TRAF2* KO in adult mice causes lethality in conjunction with enhanced hepatic necrosome formation. (**a**) Inducible *TRAF2* KO mice (*n* = 5) were injected i. p. with vehicle or tamoxifen at the indicated doses daily for 5 days followed by observation for morbidity. (**b**, **c**) Representative image of overall external (**b**) and internal abdominal cavity (**c**) condition. (**d**, **e**) WT and *TRAF2* KO mice were injected with tamoxifen as in **a**. Livers were collected 3 days after the final tamoxifen injection (day 8), extracted and analyzed for necrosome formation (**d**) and TRAF2-MLKL association (**e**) by IP and IB as indicated

weight and had to be killed or died within 3 days of final injection (day 8) (Supplementary Figures 4A–C). To determine whether necroptosis contributed to morbidity, we harvested livers from WT and *TRAF2* KO mice at day 8 and examined tissue extracts for necrosome formation. Whereas necrosome assembly was not detectable in WT livers, it was readily observable in livers from *TRAF2* KO mice (Figure 4d). Importantly, MLKL IP revealed interaction with TRAF2 in livers from WT but not *TRAF2* KO mice (Figure 4e). We were unable to measure necrosome formation in intestinal tissue extracts (Supplementary Figure 4D). Thus, *TRAF2* deletion *in vivo* causes morbidity in conjunction with enhanced hepatic necrosome formation, suggesting that excessive necroptosis might contribute to lethality.

RIPK3 KO delays TRAF2 KO mortality. To assess the latter more directly, we generated the same inducible *TRAF2* KO on a *RIPK3* KO background, by crossing *TRAF2 loxp/loxp*

RosaCre ERTS mice with *RIPK3*.neono.ko mice (see Methods). This cross did not result in gross developmental or postnatal abnormality (data not shown). However, upon induction of *TRAF2* deletion by tamoxifen (20 mg/kg per day daily over 5 days), *TRAF2/RIPK3* double-KO (DKO) mice displayed a significant delay in mortality relative to *TRAF2* KO mice, with a median survival of 99 *versus* 30 h following final tamoxifen dosing (Figures 5a–c and Supplementary Figure 4E). DKO mice did ultimately die, displaying deterioration in vital appearance of the liver and gastrointestinal system. Surprisingly, whereas intestinal tissue extracts from WT and *TRAF2* KO mice did not have detectable procaspase-8 (p55/53) protein, extracts from DKO mice showed elevated procaspase-8 as well as cleaved caspase-8 (p43/41) (Figures 5d and e). Intestinal extracts from DKO mice also showed an increase in caspase-8 mRNA levels as compared with those from WT or *TRAF2* KO mice (Supplementary Figure 4F). Consistent with this, intestinal extracts from WT
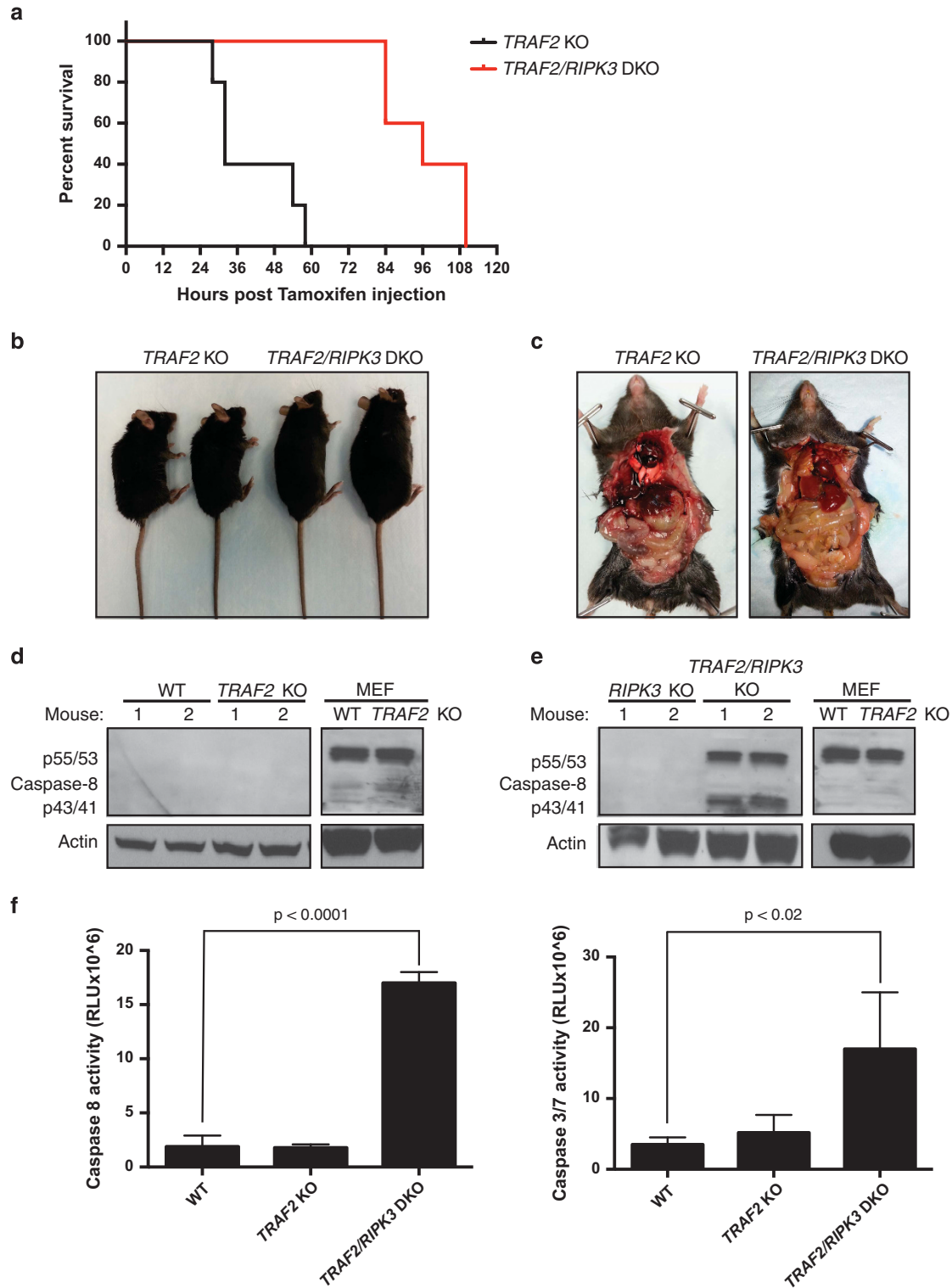
Figure 5 *RIPK3* KO delays *TRAF2* KO lethality but augments intestinal caspase-8 activity. (**a**) Mice with inducible *TRAF2* KO on a *RIPK3* WT or a *RIPK3* KO background (DKO) were injected i.p. with tamoxifen (20 mg/kg) daily for 5 days and observed for morbidity (*n* = 5, *P* = 0.006). (**b, c**) Representative image of overall external condition (**b**) and internal abdominal cavity (**c**). (**d, e**) WT and *TRAF2* KO mice (**d**) or *RIPK3* KO and *TRAF2/RIPK3* DKO mice (**e**) were injected with tamoxifen as in **a**. Intestines were collected on day 8 (or day 7 if signs of morbidity appeared) and intestinal extracts were analyzed by caspase-8 IB in comparison with equal protein amounts. (**f**) WT, *TRAF2* KO and *TRAF2/RIPK3* DKO mice were injected as in **a**. Intestinal extracts were collected as in **d** and **e** and analyzed by caspase-8 and caspase-3/7 activity assay. Bar graphs depict mean ± S.E.M. (*n* = 4). *P* values are by log-rank (Mantel-Cox) test (**a**) or Student's *t* test (**f**)

and *TRAF2* KO mice showed minimal caspase-8 and caspase-3/7 activity, whereas DKO mice displayed higher activity, especially of caspase-8 (Figure 5f). Furthermore, hepatic extracts from either mouse genotype showed little difference in total caspase-8 and caspase-3/7 levels or activity (Supplementary Figures 4G and H). Thus, although necroptosis in the liver (and perhaps other tissues not examined) may drive lethality in *TRAF2* KO mice, intestinal apoptosis may be more pathologically dominant in *TRAF2/ RIPK3* DKO mice.

Combined neutralization of death ligands differentially impacts lethality. To examine whether additional death receptors besides TNFR1, namely DR5 and Fas, mediate necroptosis *in vivo*, we used Fc-fusion decoys based on each receptor's ligand-binding ectodomain. We injected each decoy protein or a CD4-Fc control at 10 μg per day during the 5 days of tamoxifen treatment. TNFR1-Fc, DR5-Fc and Fas-Fc each delayed *TRAF2* KO lethality, extending median survival by 3, 2 or 1 day, respectively, relative to CD4-Fc (Figure 6a). Importantly, combined treatment with all three death-receptor Fc fusions fully rescued *TRAF2* KO mice from weight loss and lethality for at least 3 weeks (Figure 6b and Supplementary Figures 5A and B). Moreover, combined Fc treatment also blocked necrosome formation in the liver (Supplementary Figure 5C). In marked contrast, combined Fc administration during tamoxifen treatment did not prevent—and, at best, delayed—mortality in *TRAF2/RIPK3* DKO mice (Figure 6c). TNFR1-Fc alone or combined Fc injection similarly increased median survival from 4 to 6 days (Figures 6c and d). Together, these results suggest that upon *TRAF2* KO on a WT background, integrated death-ligand signaling is necessary and sufficient to drive mortality. In contrast, upon *TRAF2* KO on a *RIPK3* KO background, although TNFR1 signaling appears to contribute to lethality early on, other signals—independent of DR5 or Fas— eventually drive death. Previous work suggests that type I IFN promotes apoptosis independently of death ligands.[45] Injection of IFNα receptor type 1 (IFNAR1-Fc) together with TNFR1-Fc further extended survival by about 4 days (Figure 6e) and diminished caspase-8 and caspase-3/7 activity in intestinal extracts (Figure 6f). Thus, IFNAR1 significantly contributes along with TNFRI to the lethality of *TRAF2* KO on a *RIPK3*-null background, but additional pathological driver(s) must exist.

Discussion

Necroptosis appears to act as a fail-safe mechanism for apoptosis.[39,46] A number of critical mediators of necroptotic signaling downstream of death receptors have been identified, including RIPK1, RIPK3 and MLKL. Several components of the NF-κB and the cell-extrinsic apoptosis pathways, including cIAPs, CYLD and caspase-8, exert important regulatory controls on necroptotic signaling via TNFR1.[24,29] Previous work implicates TRAF2 as an adaptor that binds to TNFR1 upon ligation by TNFα and recruits cIAPs into the membrane-proximal signaling complex to promote NF-κB activation.[31,33,41,47] TRAF2 inhibits TNFα–induced apoptosis independent of its role in NF-κB activation.[40,48] TRAF2 also

suppresses death-receptor-mediated apoptosis by promoting K48-ubiquitination and proteasomal degradation of activated caspase-8.[34] The present findings demonstrate that TRAF2 plays an additional role in curbing necroptotic TNFα signaling by acting both upstream and downstream of the necrosome. Our investigation establishes an important role for TRAF2 as a necroptosis suppressor *in vitro* and *in vivo*.

TRAF2 KO in mice causes perinatal lethality that is prevented by deletion of *TNFα* or *TNFR1*.[35,36] The lethal *TRAF2* KO phenotype is diminished on a BALB/c background, though these mice succumb within 2 weeks after birth and display symptoms of inflammatory bowel disease.[37] *TRAF2*-deficient mice have exacerbated hepatocyte apoptosis and mortality upon injection with agonistic anti-Fas antibody.[34] Given its involvement in modulating apoptotic cell death, we asked whether TRAF2 also plays a significant role in regulating necroptosis.

To approach this question, we used loss-of-function strategies, including siRNA knockdown and gene KO, as well as some gain-of-function modalities. Mouse L929 fibroblasts displayed an augmented necroptotic response to TNFα, as did *TRAF2* KO MEFs. Knockdown of RIPK1, RIPK3 or MLKL reversed this augmentation, confirming an effect of TRAF2 on necroptotic signaling. *TRAF2* KO MEFs showed stronger necrosome formation than did WT MEFs, suggesting that at least one level of necroptosis suppression by TRAF2 is exerted upstream. One possible explanation for this enhanced necrosome formation is a diminished recruitment of cIAPs— and consequently—less RIPK1 ubiquitination, which would promote RIPK1 activation and necrosome assembly.[2,23,28] However, phenotypic differences between *TRAF2 versus cIAP1* KO MEFs suggested that TRAF2 may act also at some additional level(s). Several lines of evidence support this: first, endogenous TRAF2 and MLKL could be co-immuno-precipitated *in vitro* and *in vivo*. Second, whereas TRAF2 and MLKL pre-associated in untreated cells, TNFα treatment induced their dissociation—in concert with increased recruitment of MLKL to RIPK3. Third, TRAF2 and MLKL bound to each other upon ectopic co-expression. Although the RING and CIM regions of TRAF2 were dispensable for MLKL binding, the C-terminal portion, which contains the TRAF homology motif, was important. This finding reinforces the conclusion that TRAF2 and MLKL interact in a biologically specific manner. Furthermore, immunofluorescence studies showed significant co-localization of TRAF2 and MLKL in non-stimulated cells and its reversal by TNFα. MLKL overexpression was sufficient to drive cell death as previously shown;[14] consistent with the co-IP results, this was reversed by co-expression of WT *TRAF2* and the RING and CIM but not the C-terminal deletion variants. Together, these findings support the conclusion that TRAF2 exerts additional suppression of necroptosis at the level of MLKL. RIPK3 and MLKL showed significantly stronger baseline interaction in the absence of TRAF2, suggesting that TRAF2 and RIPK3 may compete for MLKL binding. Indeed, we observed substantially less binding of TRAF2 and MLKL upon co-transfection with RIPK3 in HEK293 cells (data not shown).

CYLD promotes necrosome formation by deubiquitinating RIPK1.[29] Our data unravel an important additional
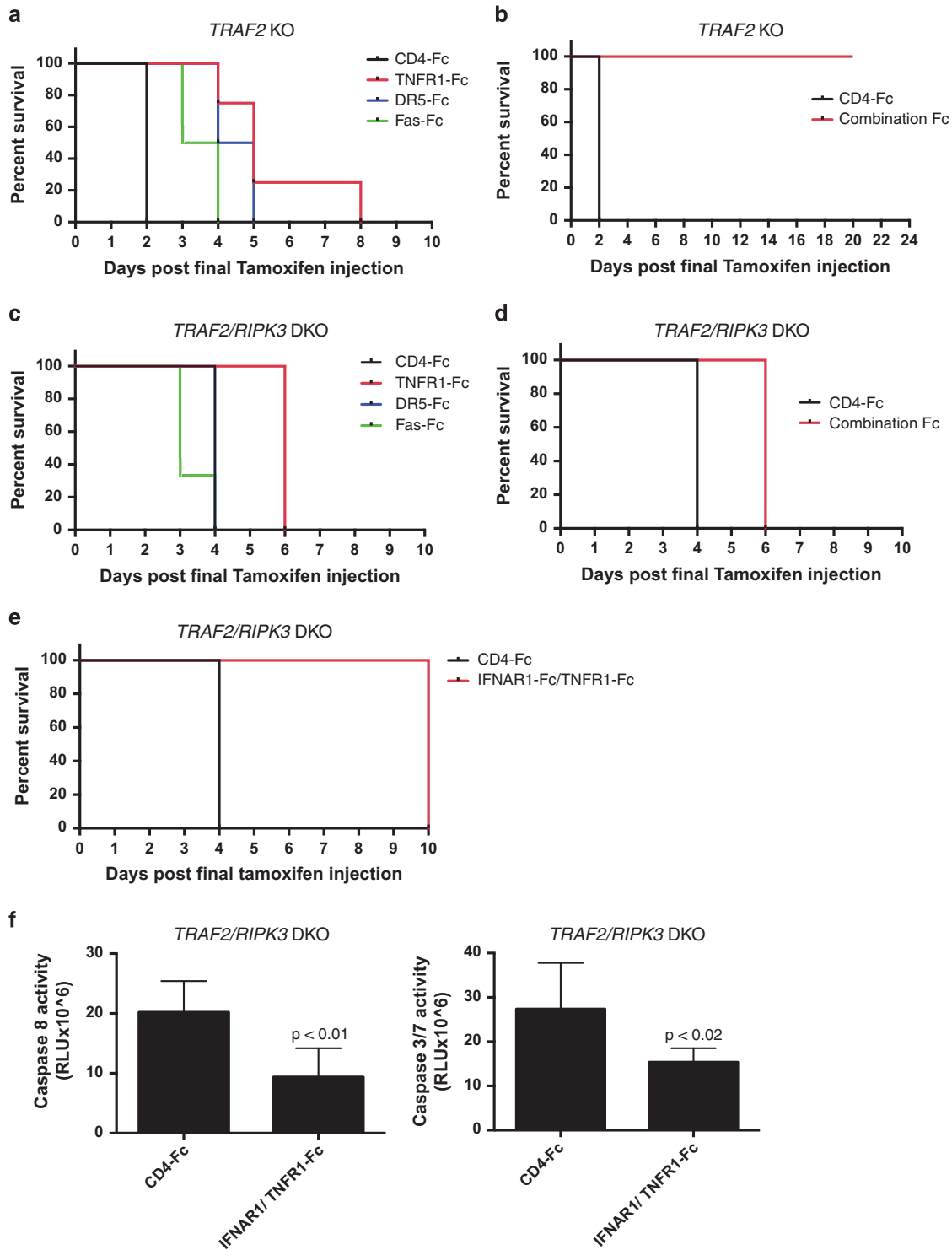
Figure 6 Death ligands differentially contribute to lethality in *TRAF2* KO and *TRAF2/RIPK3* DKO mice. (**a**) *TRAF2* KO mice were injected i.p. with tamoxifen (20 mg/kg) daily for 5 days. Mice were injected concurrently with 10 μg per mouse each of CD4-Fc, TNFR1-Fc, DR5-Fc or Fas-Fc and observed for morbidity ($n = 4$, $P = <0.0015$). (**b**) *TRAF2* KO mice were injected with tamoxifen as in **a** concurrently with control CD4-Fc (30 μg per mouse) or a combination of TNFR1-Fc, DR5-Fc and Fas-Fc (10 μg per mouse each) ($n = 3$, <0.05). (**c**) *TRAF2/RIPK3* DKO mice were treated as in **a** ($n = 3$, $P = 0.0113$). (**d**) *TRAF2/RIPK3* DKO mice were treated as in **b** ($n = 3$, $P = 0.0253$). (**e**, **f**) *TRAF2/RIPK3* DKO mice were treated with tamoxifen as in **a**, concurrently with CD4-Fc (20 μg per mouse) or TNFR1-Fc and IFNAR1-Fc (10 μg per mouse). Mice were followed for morbidity ($n = 4$, $P = 0.0082$) (**e**). Intestines were collected on day 9 and extracts were analyzed by caspase-8 and caspase-3/7 activity assay (**f**). Bar graphs depict mean $\pm$ S.E.M. ($n = 4$). *P* values are by log-rank (Mantel-Cox) test (**a**–**e**) or Student's *t* test (**f**)

pro-necroptotic function of CYLD via dequbiquitination of TRAF2. In L929 cells, TRAF2 displayed baseline ubiquitination, which was reversed in a CYLD-dependent manner upon TNFα treatment. CYLD was also required for TNFα-induced dissociation of TRAF2 from MLKL and the consequent enhancement of necroptosis. In studies with purified recombinant proteins, cIAP1-mediated ubiquitination of TRAF2 supported binding to MLKL, providing evidence for direct association, whereas CYLD-mediated deubiquitination of TRAF2 attenuated this interaction. Thus, CYLD-dependent TRAF2 deubiquitination reverses TRAF2-MLKL binding, perhaps permitting better MLKL engagement by the necrosome to trigger necroptosis.

Our *in vivo* findings support a role for TRAF2 in suppressing both apoptosis and necroptosis and demonstrate that this function is biologically critical. Whereas *TRAF2* KO in adult mice led to rapid lethality, this was significantly delayed by *RIPK3* KO, suggesting that unchecked necroptosis in the absence of *TRAF2* contributes significantly to the observed mortality. Consistent with this, *TRAF2* KO mice displayed spontaneous hepatic necrosome formation. It is likely that unchecked apoptosis also contributes to mortality upon *TRAF2* KO, particularly in the absence of *RIPK3*. Supporting this, *TRAF2*/*RIPK3* DKO mice showed a spontaneous increase in intestinal levels of caspase-8 protein and processing as well as enzymatic activity. A recent finding that may be related to this observation is that RIPK3 supports caspase-8 activation in a kinase-independent capacity.[49] It is conceivable therefore that the observed death is primarily caused by excessive hepatic necroptosis in *TRAF2* KO mice and by intestinal apoptosis in *TRAF2*/*RIPK3* DKO mice. Although access to detailed histopathological analysis was not available to us in this study, it is notable that the DKO phenotype bears similarity to that reported recently for selective *RIPK1* KO in intestinal epithelial cells.[50–52] The latter involves kinase-independent RIPK1 activity, which confers stabilization of several pro-survival proteins, including TRAF2, cIAPs and cFLIP.[52] It will be interesting to investigate whether TRAF2 is linked to the kinase-independent functions of RIPK1 and/or RIPK3.

Combined inhibition of the key death ligands TNFα, FasL and Apo2L/TRAIL using receptor-Fc decoys provided complete protection of *TRAF2* KO but not *TRAF2*/*RIPK3* DKO mice. This unexpected difference suggests that other pathological drivers may be involved in lethality upon deletion of both *TRAF2* and *RIPK3*. Previous reports suggest that type I IFN upregulates caspase-8 transcription and promotes apoptosis independent of death ligands.[45] Moreover, TRAF2 is implicated in signaling by IFNAR1.[53] In keeping with these findings, we observed diminished caspase-8 and caspase-3/7 activity in intestinal extracts from *TRAF2* KO mice treated with TNFR1-Fc plus IFNAR1-Fc. Thus, in the absence of TRAF2, type I IFN signaling may be altered in a manner that augments apoptosis via caspase-8; other factors that remain to be identified further contribute to lethality in the added absence of RIPK3. In conclusion, our findings demonstrate that TRAF2 is an important biological suppressor of both apoptosis and necroptosis, affecting homeostasis of key organs and viability of the whole organism.

Materials and Methods

Cell culture. WT, *TRAF2* KO, *cIAP1* KO MEFs and L929 cells were cultured in Dulbecco's modified Eagle's medium. Culture media was supplemented with 10% fetal bovine serum and 2 mM L-glutamine.

Experimental reagents. Abs for IP and IB analysis were TRAF2 (C-20, F-2), MLKL (Y-14), CYLD (E-10) and c-myc (9E10) from Santa Cruz, Dallas, TX, USA, RIPK1 (610459) from BD Bioscience (San Jose, CA, USA), RIPK3 (2283) from Pro-Sci (Poway, CA, USA), MLKL (clone 3H1) from Millipore (Billerica, MA, USA), ubiquitin (P4D1) from Cell Signaling (Danvers, MA, USA) and RIPK3 from Genentech (South San Francisco, CA, USA). TNFα, and recombinant CD4-, TNFR1-, DR5-, Fas-, and IFNAR1-Fc fusion proteins[54,55] were from Genentech. zVAD, cycloheximide, Necrostatin-1 and tamoxifen were from Sigma (St. Louis, MO, USA). Recombinant TRAF2 and MLKL were purchased from Novus (Littleton, CO, USA). Recombinant cIAP1 and CYLD were purchased from Boston Biochem (Cambridge, MA, USA).

Reagents, siRNA and cDNA transfection. The siRNA oligonucleotides against TRAF2, RIPK1, RIPK3, MLKL and CYLD were from Dharmacon (Lafayette, CO, USA).

Nontargeting siRNA control (siNTC, D-001810-01); GFP siRNA control (P-002048); TRAF2 (L-042814-01); RIP1 (L-040150-00); RIPK3 (L-049919-01); MLKL (L-061420-01); CYLD (L-055575-01). L929 cells were reverse-transfected using RNAiMAX from Thermo Fisher Scientific (Waltham, MA, USA). WT and *TRAF2* KO MEFs were transfected using Genemute siRNA and plasmid transfection reagent from SignaGen Laboratories (Rockville, MD, USA), all according to the manufacturer's protocol.

The expression construct for the myc-tagged MLKL and FLAG-tagged WT TRAF2 and deletion mutants lacking the RING, CIM and TRAF domains were generated by DNA synthesis or site-directed mutagenesis. For ectopic expression experiments, L929 cells were transfected using Lipofectamine LTX Plus reagent (Thermo Fisher Scientific), while MEFs were transfected using Genemate transfection reagent, both according to the manufacturer's protocol.

IP and IB analysis. Cells were grown on 15 cm plates, treated as indicated, washed with PBS, and harvested with 1 ml of the following lysis buffer: 20 mM Tris HCL (pH 7.5), 150 mM NaCl, 1.5% Triton X-100, plus protease and phosphatase inhibitors from Roche Diagnostics (Indianapolis, IN, USA).

Cell extracts were left on ice for 20 min and centrifuged at 14 000 r.p.m. for 15 min. Five milligrams of protein lysate were used for IP using 2 μg of the following antibodies: RIPK1 (610459), RIPK3 (Genentech), MLKL (clone 3H1) and TRAF2 (F-2) for overnight at 4 °C. The following day, 25 μl of protein A/G ultralink resin from Thermo Fisher Scientific was added for 2 h at 4 °C, and the IPs were washed three times with lysis buffer, sample buffer was added, and beads were boiled for 5 min at 95 °C. Samples were then analyzed by SDS-PAGE followed by IB.

Analysis of ubiquitination. For analysis of total TRAF2 ubiquitylation, 1.5% SDS and was added to cell lysates (5 mg protein), boiled for 15 min at 95 °C, diluted to 0.15% SDS lysis buffer and subjected to IP utilizing 10ug TRAF2 (F-2) IP antibody and 100 ul protein A/G ultralink resin (Thermo Fisher Scientific) and then analyzed as above.

***In vitro* ubiquitination of TRAF2 and binding to MLKL.** Recombinant TRAF2 (60 ng) was added to a ubiquitination reaction mix (30 μl) containing E1, E2, cIAP1 and ubiquitin, as per manufacturer's instructions (Boston Biochem) and incubated for 1 h. Recombinant MLKL (60 ng) and CYLD (60 ng) were added as indicated, and incubation was continued at 37 °C for an additional 1 h. To stop the reaction, 1 ml lysis buffer containing TRAF2 antibody was added for 1 h at room temperature, followed by the addition of protein A/G ultralink resin for another 1 h. Beads were washed three times with lysis buffer, eluted and analyzed by SDS-PAGE.

Generation of inducible TRAF2/RIPK3 DKO mice. *TRAF2* loxp/loxp RosaCre ERTS mice and *RIPK3*.neono.ko mice were generated as previously described.[56] To create *TRAF2* KO/*RIPK3* DKO mice, the two lines were crossed and mice were screened for TRAF2 loxp/loxp sites targeting exon 3 of TRAF2 and for Rosa-creERT2, as well as for *RIPK3* KO.

To induce *TRAF2* KO, tamoxifen was solubilized in sunflower oil and administered by intraperitoneal injection at the indicated dosages for five consecutive days followed

by observation. Fc-fusion proteins were diluted in PBS at a concentration of 100 μg/ml and each mouse was dosed with 10 μg total protein concurrently with tamoxifen by intraperitoneal injection.

All procedures were approved by and conformed to the guidelines and principles set by the Institutional Animal Care and Use Committee of Genentech and were carried out in an Association for the Assessmentand Accreditation of Laboratory Animal Care (AAALAC)-accredited facility.

Immunocytochemistry and confocal microscopy. L929 cells grown on Lab-TekII chamberslides from Thermo Fisher Scientific were preincubated in the presence or absence of cycloheximide and zVAD for 30 min at 37 °C and then treated with or without TNFα for 90 min. Cultures were fixed with 4% paraformaldehyde for 15 min at room temperature and permeabilized with 0.2% saponin in blocking buffer (10% goat serum, 10 mM Hepes, 10 mM glycine in RPMI 1640) for 15 min at room temperature. Slides were then washed and blocked in blocking buffer for 1h at room temperature. Anti-MLKL (1 : 200), anti-TRAF2 (1 : 500) and anti-RIPK3 (1 : 50) were diluted in blocking buffer incubated with cells at 4 °C overnight. After three washes with PBS, cells were incubated with respective 1 : 200 diluted secondary antibodies conjugated with either Alexa488, Alexa555 or Alexa647 (Invitrogen). Slides were mounted with Prolong Gold anti-fade reagent containing DAPI from Thermo Fisher Scientific and viewed with a LEICA (Buffalo Grove, IL, USA) SP5 inverted confocal microscope under a × 63 oil objective, using Leica LAS AF software to acquire images.

Quantitation of co-localized signal. Images were collected randomly (six images from each treatment; three independent experiments), and colocalization was determined with the 'Colocalization' Plug-in of ImageJ (NIH) with the same color-threshold settings for all six images from each treatment. The co-localized color channel (two of the three colors (red, green and blue)) were then counted with the 'Analyze particles' command of Image J. Percent colocalization was then calculated by total area of co-localized channel over total area of both channels.

Analysis of caspase-8 mRNA expression. Intestinal extracts were harvested and total RNA was extracted utilizing RNeasy Plus Mini kit (Qiagen, Valencia, CA, USA). RNA was converted to cDNA utilizing RT2 First Strand kit from Qiagen. Real-time PCR was then performed using RT2 qPCR primers for caspase-8, actin and GAPDH (Qiagen) on an Applied Biosystems (Waltham, MA, USA) ViiA7 qPCR machine.

Conflict of Interest

The authors declare no conflict of interest.

1. Zhang DW, Shao J, Lin J, Zhang N, Lu BJ, Lin SC *et al*. RIP3, an energy metabolism regulator that switches TNF-induced cell death from apoptosis to necrosis. *Science* 2009; **325**: 332–336.
2. He S, Wang L, Miao L, Wang T, Du F, Zhao L *et al*. Receptor interacting protein kinase-3 determines cellular necrotic response to TNF-alpha. *Cell* 2009; **137**: 1100–1111.
3. Ashkenazi A, Salvesen G. Regulated cell death: signaling and mechanisms. *Annu Rev Cell Dev Biol* 2014; **30**: 337–356.
4. Salvesen GS, Ashkenazi A. Snapshot: caspases. *Cell* 2011; **147**: 476–e1.
5. Cho YS, Challa S, Moquin D, Genga R, Ray TD, Guildford M *et al*. Phosphorylation-driven assembly of the RIP1-RIP3 complex regulates programmed necrosis and virus-induced inflammation. *Cell* 2009; **137**: 1112–1123.
6. Zhao J, Jitkaew S, Cai Z, Choksi S, Li Q, Luo J *et al*. Mixed lineage kinase domain-like is a key receptor interacting protein 3 downstream component of TNF-induced necrosis. *Proc Natl Acad Sci U S A* 2012; **109**: 5322–5327.
7. Robinson N, McComb S, Mulligan R, Dudani R, Krishnan L, Sad S. Type I interferon induces necroptosis in macrophages during infection with Salmonella enterica serovar Typhimurium. *Nat Immunol* 2012; **13**: 954–962.
8. Mocarski ES, Upton JW, Kaiser WJ. Viral infection and the evolution of caspase 8-regulated apoptotic and necrotic death pathways. *Nat Rev Immunol* 2012; **12**: 79–88.
9. Li J, McQuade T, Siemer AB, Napetschnig J, Moriwaki K, Hsiao YS *et al*. The RIP1/RIP3 necrosome forms a functional amyloid signaling complex required for programmed necrosis. *Cell* 2012; **150**: 339–350.
10. Murphy JM, Czabotar PE, Hildebrand JM, Lucet IS, Zhang JG, Alvarez-Diaz S *et al*. The pseudokinase MLKL mediates necroptosis via a molecular switch mechanism. *Immunity* 2013; **39**: 443–453.
11. Sun L, Wang H, Wang Z, He S, Chen S, Liao D *et al*. Mixed lineage kinase domain-like protein mediates necrosis signaling downstream of RIP3 kinase. *Cell* 2012; **148**: 213–227.
12. Wang H, Sun L, Su L, Rizo J, Liu L, Wang LF *et al*. Mixed lineage kinase domain-like protein MLKL causes necrotic membrane disruption upon phosphorylation by RIP3. *Mol Cell* 2014; **54**: 133–146.
13. Galluzzi L, Kepp O, Kroemer G. MLKL regulates necrotic plasma membrane permeabilization. *Cell Res* 2014; **24**: 139–140.
14. Dondelinger Y, Declercq W, Montessuit S, Roelandt R, Goncalves A, Bruggeman I *et al*. MLKL compromises plasma membrane integrity by binding to phosphatidylinositol phosphates. *Cell Rep* 2014; **7**: 971–981.
15. Chen X, Li W, Ren J, Huang D, He WT, Song Y *et al*. Translocation of mixed lineage kinase domain-like protein to plasma membrane leads to necrotic cell death. *Cell Res* 2014; **24**: 105–121.
16. Zhou W, Yuan J. Necroptosis in health and diseases. *Semin Cell Dev Biol* 2014; **35**: 14–23.
17. Linkermann A, Hackl MJ, Kunzendorf U, Walczak H, Krautwald S, Jevnikar AM. Necroptosis in immunity and ischemia-reperfusion injury. *Am J Transplant* 2013; **13**: 2797–2804.
18. Linkermann A, Brasen JH, Himmerkus N, Liu S, Huber TB, Kunzendorf U *et al*. Rip1 (receptor-interacting protein kinase 1) mediates necroptosis and contributes to renal ischemia/reperfusion injury. *Kidney Int* 2012; **81**: 751–761.
19. Welz PS, Wullaert A, Vlantis K, Kondylis V, Fernandez-Majada V, Ermolaeva M *et al*. FADD prevents RIP3-mediated epithelial cell necrosis and chronic intestinal inflammation. *Nature* 2011; **477**: 330–334.
20. Oberst A, Dillon CP, Weinlich R, McCormick LL, Fitzgerald P, Pop C *et al*. Catalytic activity of the caspase-8-FLIP(L) complex inhibits RIPK3-dependent necrosis. *Nature* 2011; **471**: 363–367.
21. Kaiser WJ, Upton JW, Long AB, Livingston-Rosanoff D, Daley-Bauer LP, Hakem R *et al*. RIP3 mediates the embryonic lethality of caspase-8-deficient mice. *Nature* 2011; **471**: 368–372.
22. Bonnet MC, Preukschat D, Welz PS, van Loo G, Ermolaeva MA, Bloch W *et al*. The adaptor protein FADD protects epidermal keratinocytes from necroptosis in vivo and prevents skin inflammation. *Immunity* 2011; **35**: 572–582.
23. Vanlangenakker N, Vanden Berghe T, Bogaert P, Laukens B, Zobel K, Deshayes K *et al*. cIAP1 and TAK1 protect cells from TNF-induced necrosis by preventing RIP1/RIP3-dependent reactive oxygen species production. *Cell Death Differ* 2011; **18**: 656–665.
24. O'Donnell MA, Perez-Jimenez E, Oberst A, Ng A, Massoumi R, Xavier R *et al*. Caspase 8 inhibits programmed necrosis by processing CYLD. *Nat Cell Biol* 2011; **13**: 1437–1442.
25. Wu J, Huang Z, Ren J, Zhang Z, He P, Li Y *et al*. Mlkl knockout mice demonstrate the indispensable role of Mlkl in necroptosis. *Cell Res* 2013; **23**: 994–1006.
26. Bertrand MJ, Milutinovic S, Dickson KM, Ho WC, Boudreault A, Durkin J *et al*. cIAP1 and cIAP2 facilitate cancer cell survival by functioning as E3 ligases that promote RIP1 ubiquitination. *Mol Cell* 2008; **30**: 689–700.
27. Rodrigue-Gervais IG, Labbe K, Dagenais M, Dupaul-Chicoine J, Champagne C, Morizot A *et al*. Cellular inhibitor of apoptosis protein cIAP2 protects against pulmonary tissue necrosis during influenza virus infection to promote host survival. *Cell Host Microbe* 2014; **15**: 23–35.
28. Jacquel A, Auberger P. cIAPs and XIAP reduce RIPKs to silence. *Blood* 2014; **123**: 2445–2446.
29. Moquin DM, McQuade T, Chan FK. CYLD deubiquitinates RIP1 in the TNFalpha-induced necrosome to facilitate kinase activation and programmed necrosis. *PLoS One* 2013; **8**: e76841.
30. Vince JE, Pantaki D, Feltham R, Mace PD, Cordier SM, Schmukle AC *et al*. TRAF2 must bind to cellular inhibitors of apoptosis for tumor necrosis factor (tnf) to efficiently activate nf-{kappa}b and to prevent tnf-induced apoptosis. *J Biol Chem* 2009; **284**: 35906–35915.
31. Shu HB, Takeuchi M, Goeddel DV. The tumor necrosis factor receptor 2 signal transducers TRAF2 and c-IAP1 are components of the tumor necrosis factor receptor 1 signaling complex. *Proc Natl Acad Sci U S A* 1996; **93**: 13973–13978.
32. Hsu H, Shu HB, Pan MG, Goeddel DV. TRADD-TRAF2 and TRADD-FADD interactions define two distinct TNF receptor 1 signal transduction pathways. *Cell* 1996; **84**: 299–308.
33. Rothe M, Sarma V, Dixit VM, Goeddel DV. TRAF2-mediated activation of NF-kappa B by TNF receptor 2 and CD40. *Science* 1995; **269**: 1424–1427.
34. Gonzalvez F, Lawrence D, Yang B, Yee S, Pitti R, Marsters S *et al*. TRAF2 Sets a threshold for extrinsic apoptosis by tagging caspase-8 with a ubiquitin shutoff timer. *Mol Cell* 2012; **48**: 888–899.
35. Yeh WC, Shahinian A, Speiser D, Kraunus J, Billia F, Wakeham A *et al*. Early lethality, functional NF-kappaB activation, and increased sensitivity to TNF-induced cell death in TRAF2-deficient mice. *Immunity* 1997; **7**: 715–725.
36. Lee SY, Reichlin A, Santana A, Sokol KA, Nussenzweig MC, Choi Y. TRAF2 is essential for JNK but not NF-kappaB activation and regulates lymphocyte proliferation and survival. *Immunity* 1997; **7**: 703–713.
37. Piao JH, Hasegawa M, Heissig B, Hattori K, Takeda K, Iwakura Y *et al*. Tumor necrosis factor receptor-associated factor (TRAF) 2 controls homeostasis of the colon to prevent

spontaneous development of murine inflammatory bowel disease. *J Biol Chem* 2011; **286**: 17879–17888.

38. Karl I, Jossberger-Werner M, Schmidt N, Horn S, Goebeler M, Leverkus M *et al.* TRAF2 inhibits TRAIL- and CD95L-induced apoptosis and necroptosis. *Cell Death Dis* 2014; **5**: e1444.

39. Vandenabeele P, Galluzzi L, Vanden Berghe T, Kroemer G. Molecular mechanisms of necroptosis: an ordered cellular explosion. *Nat Rev Mol Cell Biol* 2010; **11**: 700–714.

40. Gentle IE, Wong WW, Evans JM, Bankovacki A, Cook WD, Khan NR *et al.* In TNF-stimulated cells, RIPK1 promotes cell survival by stabilizing TRAF2 and cIAP1, which limits induction of non-canonical NF-kappaB and activation of caspase-8. *J Biol Chem* 2011; **286**: 13282–13291.

41. Takeuchi M, Rothe M, Goeddel DV. Anatomy of TRAF2. Distinct domains for nuclear factor-kappaB activation and association with tumor necrosis factor signaling proteins. *J Biol Chem* 1996; **271**: 19935–19942.

42. Sondarva G, Kundu CN, Mehrotra S, Mishra R, Rangasamy V, Sathyanarayana P *et al.* TRAF2-MLK3 interaction is essential for TNF-alpha-induced MLK3 activation. *Cell Res* 2010; **20**: 89–98.

43. Kovalenko A, Chable-Bessia C, Cantarella G, Israel A, Wallach D, Courtois G. The tumour suppressor CYLD negatively regulates NF-kappaB signalling by deubiquitination. *Nature* 2003; **424**: 801–805.

44. Trompouki E, Hatzivassiliou E, Tsichritzis T, Farmer H, Ashworth A, Mosialos G. CYLD is a deubiquitinating enzyme that negatively regulates NF-kappaB activation by TNFR family members. *Nature* 2003; **424**: 793–796.

45. Lietke CG N, Manns M, Trautwein C. Interferon-alpha enhances TRAIL-mediated apoptosis by up-regulating caspase-8 transcription in human hepatoma cells. *J Hepatol* 2006; **44**: 342–349.

46. Linkermann A, Green DR. Necroptosis. *N Engl J Med* 2014; **370**: 455–465.

47. Hsu H, Huang J, Shu HB, Baichwal V, Goeddel DV. TNF-dependent recruitment of the protein kinase RIP to the TNF receptor-1 signaling complex. *Immunity* 1996; **4**: 387–396.

48. Wong WW, Gentle IE, Nachbur U, Anderton H, Vaux DL, Silke J. RIPK1 is not essential for TNFR1-induced activation of NF-kappaB. *Cell Death Differ* 2010; **17**: 482–487.

49. Newton K, Dugger DL, Wickliffe KE, Kapoor N, de Almagro MC, Vucic D *et al.* Activity of protein kinase RIPK3 determines whether cells die by necroptosis or apoptosis. *Science* 2014; **343**: 1357–1360.

50. Rickard JA, O'Donnell JA, Evans JM, Lalaoui N, Poh AR, Rogers T *et al.* RIPK1 regulates RIPK3-MLKL-driven systemic inflammation and emergency hematopoiesis. *Cell* 2014; **157**: 1175–1188.

51. Takahashi N, Vereecke L, Bertrand MJ, Duprez L, Berger SB, Divert T *et al.* RIPK1 ensures intestinal homeostasis by protecting the epithelium against apoptosis. *Nature* 2014; **513**: 95–99.

52. Dannappel M, Vlantis K, Kumari S, Polykratis A, Kim C, Wachsmuth L *et al.* RIPK1 maintains epithelial homeostasis by inhibiting apoptosis and necroptosis. *Nature* 2014; **513**: 90–94.

53. Yang CH, Murti A, Pfeffer SR, Fan M, Du Z, Pfeffer LM. The role of TRAF2 binding to the type I interferon receptor in alternative NF kappaB activation and antiviral response. *J Biol Chem* 2008; **283**: 14309–14316.

54. Ashkenazi A, Marsters SA, Capon DJ, Chamow SM, Figari IS, Pennica D *et al.* Protection against endotoxic shock by a tumor necrosis factor receptor immunoadhesin. *Proc Natl Acad Sci U S A* 1991; **88**: 10535–10539.

55. Ashkenazi A, Chamow SM. Immunoadhesins as research tools and therapeutic agents. *Curr Opin Immunol* 1997; **9**: 195–200.

56. Newton K, Sun X, Dixit VM. Kinase RIP3 is dispensable for normal NF-kappa Bs, signaling by the B-cell and T-cell receptors, tumor necrosis factor receptor 1, and Toll-like receptors 2 and 4. *Mol Cell Biol* 2004; **24**: 1464–1469.

Supplementary Information accompanies this paper on Cell Death and Differentiation website (http://www.nature.com/cdd)